PHYSICAL REVIEW E **70**, 045203(R) (2004)

Chaos-induced escape over a potential barrier

L. Y. Chew,[1] Christopher Ting,[2] and C. H. Lai[1]
[1]*Department of Physics, National University of Singapore, Singapore 117542*
[2]*Singapore Management University, Singapore 259756*
(Received 16 December 2003; published 29 October 2004)

We investigate the statistical parity of a class of chaos-generated noises on the escape of strongly damped particles out of a potential well. We show that statistical asymmetry in the chaotic fluctuations can lead to a skewed Maxwell–Boltzmann distribution in the well. Depending on the direction of skew, the Kramers escape rate is enhanced or suppressed accordingly. Based on the Perron–Frobenious equation, we determine an analytical expression for the escape rate's prefactor that accounts for this effect. Furthermore, our perturbative analysis proves that in the zeroth-order limit, the rate of particle escape converges to the Kramers rate.

DOI: 10.1103/PhysRevE.70.045203 PACS number(s): 05.45.−a, 05.40.−a, 02.50.−r, 82.20.−w

Thermally activated escape from metastable states, or the study of the transition of a particle over a potential barrier, is known as the Kramers problem. Kramers, in his work [1], derived the escape rate of such a particle in a potential well interacting with a heat bath of equilibrium fluctuations. The escape rate was found to have the form of an Arrhenius equation, but with a prefactor that depends on whether the interaction is moderate-to-strongly coupled (strong friction regime) or weakly coupled (weak friction regime) to the heat bath.

The Kramers problem has, since then, continued to attract growing interest [2,3]. In particular, the escape rate problem in complex nonequilibrium systems, which typically lack the property of detailed balance, has recently spurred many theoretical investigations [4]. These research studies have arisen from the urge to understand the physical processes and transport properties of noise-assisted ratchet mechanisms, with the hope of gaining insights into how useful work can be extracted from nonequilibrium fluctuations. Diverse physical examples of such systems under examination include molecular motors [5], kinetics of ligand binding to proteins [6], surface electromigration [7], and cold atoms in optical lattice [8].

Within the class of nonequilibrium systems, a chaos-driven system is one of the most important for a better understanding of the Kramers problem. Such a system interacts with an environment that displays nontrivial low-dimensional dynamics, with examples coming from a chemically reactive system that operates in a medium under hydrodynamic flow, or the turbulent transport of minute atmospheric particles [9,10]. In fact, such a system can also be created out of nanoscale devices [11]. Despite its importance, systems driven by chaos are still relatively unexplored, especially with respect to the Kramers problem, as most research on particle escape from stationary metastable nonequilibrium systems are carried out based on stochastic noise.

We attempt to fill this gap by developing a theory of escape rates for a class of chaotic nonequilibrium fluctuations acting on strongly damped particles. The theory will enable us to determine an analytical form of the escape rate, including both the prefactor and the exponent. Moreover, it will also help us to quantify the asymmetric effects of the chaotic noise on the rate of particle escape.

Let us consider a simple model of a Brownian particle in a potential $V(x)$ being subjected to periodic impulsive kick F_n at a frequency $1/\tau$, with n being the discrete time stamp. The particle is, in addition, being acted upon by a viscous force. Then, the phase-space trajectory of the Brownian particle (p_n, x_n) can be described by the following quasistationary kicked particle (QKP) map in the strong friction regime [12]:

$$F_{n+1} = G^{(N)}(F_n), \tag{1}$$

$$p_{n+1} = e^{-\gamma\tau} p_n - \frac{V'(x_n)}{\gamma}\varphi + (\gamma\tau)^{1/2} s F_{n+1}, \tag{2}$$

$$x_{n+1} = x_n + \frac{\varphi}{\gamma} p_n - \frac{V'(x_n)}{\gamma}\left(\tau - \frac{1}{\gamma}\varphi\right), \tag{3}$$

where $\varphi = 1 - e^{-\gamma\tau}$, with γ being the damping constant. The scaling factor s^2 gives the intensity of the noise, which we denote as $s^2 = 4kT$, with k being the Boltzmann constant and T the temperature. The purported "heat" source $G^{(N)}$ is, specifically, the Tchebyscheff map of order N. It is well known that the probability distribution function of these one-dimensional maps are non-Gaussian [13]. Employing the symbol $\langle \cdot \rangle$ to denote the expectation with respect to the invariant measure $h(\cdot)$ of the dynamics of $G^{(N)}$, we have for all i and j,

$$\langle F_j \rangle = 0; \quad \langle F_i F_j \rangle = \frac{1}{2}\delta(i,j). \tag{4}$$

The interest in a heat source out of iterates of Tchebyscheff maps results from its ergodic, mixing, and chaotic nature [13]. A map of order N possesses a positive Lyapunov exponent of ln N. By treating τ as a fluctuation time scale of the system, the Kolmogorov–Sinai entropy of the heat bath turns out to be ln N/τ, which approaches infinity as $\tau \to 0$, showing that a single fast chaotic degree of freedom is able to generate stochasticity [14]. In this context of vanishing time scale, it is remarkable that Tchebyscheff maps dynamics are able to induce a Brownian motion in the case of free field

[15]. After all, determinism has not disappeared with the emergence of stochastic behavior. It has simply been relegated when the time scale is infinitesimally small. By increasing the interval τ of the chaotic kicks, the predictability time scale of the system is raised and deterministic effects will become more apparent [16]. The consequence of such a change in time scale, which is to be addressed appropriately by our discrete-time model, serves to capture the effects of physical systems far from thermodynamic equilibrium, such as the Rayleigh–Bénard system with convection rolls [17] and systems undergoing turbulent flow [10].

A mathematically convenient feature of fluctuations from Tchebyscheff maps is that all its correlation properties are known [18],

$$\left\langle \prod_{i=1}^{r} F_{n_i} \right\rangle = \left(\frac{1}{2}\right)^r \sum_{\sigma} \delta\left(\sum_{i=1}^{r} \sigma_i N^{n_i}, 0 \right), \tag{5}$$

where Σ_σ is the summation over all possible configurations $(\sigma_1, \ldots, \sigma_r)$, with $\sigma_i = \pm 1$. Note that Eq. (4) is a special case of Eq. (5) and the first two correlations correspond to that of white Gaussian noise. Although the rest of its higher-order correlations are different from the white Gaussian model, they are nonetheless close to it compared to those generated by any other smooth chaotic system. Furthermore, for this class of map, the odd-order correlations exist when N is even, but all vanish when N is odd [19]. Thus, fluctuations from the odd-order Tchebyscheff maps are said to be statistically symmetric, while those from the even-order Tchebyscheff maps are statistically asymmetric [20,21]. These dissimilarities in correlation properties from other colored noise models considered for the Kramers problem [2,9] have made the Tchebyscheff maps an interesting fluctuation model for the investigation of the escape rate problem.

To examine this problem, let us apply the theoretical formalism in [12,22] to obtain the escape rate. In the overdamped limit, the QKP map is simplified to the following form:

$$F_{n+1} = G^{(N)}(F_n), \tag{6}$$

$$x_{n+1} = x_n + \left(\frac{\tau}{\gamma}\right)^{1/2} sF_n - \left(\frac{\tau}{\gamma}\right) V'(x_n). \tag{7}$$

Let us assume the perturbative ansatz $\rho(F,x,t) = \rho^{(0)}(F,x,t) + \Sigma_{i=1}^{\infty} (\tau/\gamma)^{i/2} q^{(i)}(F,x,t)$, such that $\rho^{(0)}$ is the zeroth-order probability density, while the $q^{(i)}$'s are the ith order correction terms. By means of the Perron–Frobenius approach, the behavior of an ensemble of particles given by (6) and (7) satisfies the associated inhomogeneous Smoluchowski equation,

$$\frac{kT}{\gamma} \frac{\partial^2 P_1}{\partial x^2} + \frac{\partial}{\partial x}\left(\frac{V'(x) P_1}{\gamma} \right) - \frac{\partial P_1}{\partial t} = \tau^{1/2} \gamma^{-3/2} \left(\frac{\partial \Psi}{\partial x} \right), \tag{8}$$

where $\Psi(x,t) = \int_{-1}^{1} dFsFq^{(2)}(F,x,t)$. Note that τ/γ is the perturbative parameter, while $P_1(x,t)$ is the first-order position probability distribution. Also, Eq. (8) is applicable only to Tchebyscheff maps of even order, as $\rho^{(1)}$ is separable in this case: $\rho^{(1)} = h(F) P_1(x,t)$, with $P_1(x,t) = P_0(x,t) + (\tau/\gamma)^{1/2} Q_1(x,t)$.

Before determining the escape rate from (8), let us consider the situation where the particle is caught at the bottom of a harmonic potential well $V(x) = \omega x^2/2$. In the steady state, we expect $\partial P_1(x,t)/\partial t = 0$. Hence, (8) can be solved to obtain

$$\frac{kT}{\gamma} \frac{\partial P_1}{\partial x} + \frac{V'(x)}{\gamma} P_1 = \tau^{1/2} \gamma^{-3/2} \Psi - J, \tag{9}$$

where J is the probability current corresponding to $\partial P_1(x,t)/\partial t = -\partial J/\partial x$, and it is a constant in the steady state. For a harmonic potential, J must vanish, as the potential diverges to an infinite high positive value as $x \to \pm\infty$, which indicates that the boundary is asymptotically reflective [23]. These conditions yield

$$P_1(x) = \left[\sqrt{\frac{\omega}{2\pi kT}} + \left(\frac{\tau}{\gamma}\right)^{1/2} \frac{\Phi(x)}{kT} \right] \exp\left(-\frac{\omega x^2}{2kT} \right), \tag{10}$$

where $\Phi(x) = \int_{-\infty}^{x} \exp(\omega y^2/2kT) \Psi(y) dy$. Consequently, the ensemble of particles, instead of thermalizing to the usual Maxwell–Boltzmann distribution, settles down to a perturbatively modified version within the harmonic potential well. An underlying microscopic, statistically asymmetric, fluctuation has thus led to a macroscopic asymmetric position distribution. In obtaining (10), we have used the normalization condition $\int_{-\infty}^{\infty} P_1(x) dx = 1$ and $\int_{-\infty}^{\infty} Q_1(x) dx = 0$, as $Q_1(x)$ is a correction term. In fact, the latter condition implies $\Phi(-x) = -\Phi(-x)$.

Next, let us turn to the Kramers problem. Assuming that the height of the potential barrier μ is large compared with the intensity of the chaotic noise kT, the particles will equilibrate in the neighborhood of the potential minimum at x_0, also known as the metastable state, according to the "perturbed" Maxwell–Boltzmann distribution given by (10). This ensues from adopting Kramers' assumption [1,24] that $V(x)$ is dominated by the parabolic part $\omega x^2/2$ at the metastable state. This assumption also applies to the transition state, which occurs at the top of the potential barrier at x_1. Suppose further that the transition state represents an absorbing boundary. Then, a boundary condition for $P_1(x)$ is $P_1(x_1) = 0$ [23].

The barrier escape rate is given by $K_r = J/n_0$ [1], where J is the probability current and $n_0 = \int_{x_0-\epsilon}^{x_0+\epsilon} P_1(x) dx$, with ϵ being a small number. When $\mu \gg kT$, n_0 can be suitably approximated by $n_0 \approx \int_{-\infty}^{\infty} P_1(x) dx = 1$. As a result, K_r depends essentially on J. This stationary current is maintained by sources that supply the potential well with particles having energies of the order kT, while being absorbed by sinks at the transition state [2]. Solving (9) for J with the absorbing boundary condition, we obtain

$$K_r = \frac{1}{C} \left\{ \frac{kT}{\gamma} P_1(x_0) + \tau^{1/2} \gamma^{-3/2} \int_{x_0}^{x_1} \exp\left(\frac{V(x)}{kT} \right) \Psi(x) dx \right\}, \tag{11}$$

where $C = \int_{x_0}^{x_1} \exp(V(x)/kT) dx$. In view of $\mu \gg kT$, $C \approx \exp(\mu/kT) \int_{-\infty}^{\infty} \exp[-\omega(x-x_1)^2/2kT] dx \approx \exp(\mu/kT)$

$\times\sqrt{2\pi kT/\omega}$ and $P_1(x_0)=\sqrt{\omega/(2\pi kT)}$ from (10), the escape rate due to chaotic fluctuating forces from even-order Tchebyscheff maps is given by

$$K_r = \left\{1 + \left(\frac{\tau}{\gamma}\right)^{1/2}\sqrt{\frac{2\pi}{\omega kT}}\int_{x_0}^{x_1}\exp\left(\frac{V(x)}{kT}\right)\Psi(x)dx\right\} \times \frac{\omega}{2\pi\gamma}\exp\left(-\frac{\mu}{kT}\right). \quad (12)$$

Equation (12) is the central result of this paper. It shows that the escape rate preserves the Arrhenius form even though the source of fluctuations is chaotic and non-Brownian, in contrast to escape rates due to other chaotic noise [9]. Although this is only true for perturbatively small τ/γ, it is rather surprising as the noise is intrinsically deterministic. Furthermore, when $\tau/\gamma\rightarrow 0$, the prefactor of K_r approaches one, indicating a convergence to the Kramers escape rate at the strong friction regime.

To illustrate our result, we select the second-order Tchebyscheff map as our fluctuating force. In this instance, the function $\Psi(x)$ is given by

$$\Psi(x) = \sqrt{\frac{\omega}{2\pi}}\exp\left(-\frac{V(x)}{kT}\right)\left[\frac{V'(x)^2}{kT} - V''(x)\right]. \quad (13)$$

In lieu of Kramers' parabolic approximations, we consider the potential

$$V_p(x) = \begin{cases} \frac{1}{2}\omega x^2 & \text{for } x \leqslant 0.5, \\ \mu - \frac{1}{2}\omega(x-1)^2 & \text{for } x > 0.5. \end{cases} \quad (14)$$

We restrict $\omega=4\mu$ such that as μ increases, the transition state is maintained at $x_1=1$ while the two parabolic curves are continuously connected. These conditions result in $\int_0^1 \exp[V_p(x)/kT]\Psi(x)dx=\omega^{\frac{5}{2}}/(12\sqrt{2\pi}kT)$. Thus, for the $G^{(2)}$ map, the escape rate is of the following explicit form:

$$K_r = \left\{1 + \frac{4}{3}\left(\frac{\tau}{\gamma}\right)^{1/2}\frac{\mu^2}{(kT)^{3/2}}\right\}\frac{\omega}{2\pi\gamma}\exp\left(-\frac{\mu}{kT}\right). \quad (15)$$

The necessity to fix the potential between x_0 and x_1 in order to obtain the exact prefactor up to first order reflects the non-Markovian and deterministic nature of the fluctuations. The additional term $A=(4/3)(\tau/\gamma)^{1/2}[\mu^2/(kT)^{3/2}]$ in the prefactor, as well as the corresponding one in (12), is a consequence of these properties. Moreover, with $A>0$, the deterministic $G^{(2)}$ chaotic noise has the effect of enhancing the escape rate over the conventional Kramers rate, unlike results from other colored noise models, which typically show an escape rate suppression [9,2].

From a qualitative perspective, the enhancement of the Kramers escape rate can be understood to arise from the statistical asymmetry of the noise. In the context of white Gaussian noise (which is statistically symmetric), the classical theory predicts a quick thermalization of the ensemble of particles to the Maxwell–Boltzmann distribution in the well, while the nonequilibrium condition creates a diffusion current over the transition state. In the case of chaotic fluctuations due to even-order Tchebyscheff maps, thermalization also takes place, albeit with a Maxwell–Boltzmann distribution that is perturbed by a correction term that is an odd function of x. This asymmetry in the distribution, as apparent

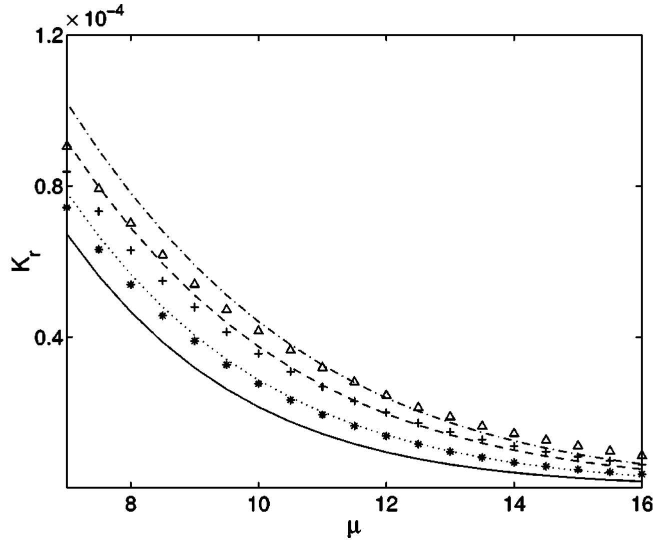

FIG. 1. The escape rate vs μ for $G^{(2)}$ map chaotic fluctuations with potential given by (14) based on analytical expression (15) (dashed-dotted, dashed, and dotted curves correspond to $\tau=1.0$, $\tau=0.5$, and $\tau=0.1$, respectively) and numerical simulation (Δ, +, and * markers correspond to $\tau=1.0$, $\tau=0.5$, and $\tau=0.1$, respectively). Kramers' rate $K_r=(\omega/2\pi\gamma)\exp(-\mu/kT)$ is given by the solid curve. The parameters employed are: $\gamma=2\times10^3$, $kT=2.0$. An ensemble size of 1×10^5 is used for the numerical simulations

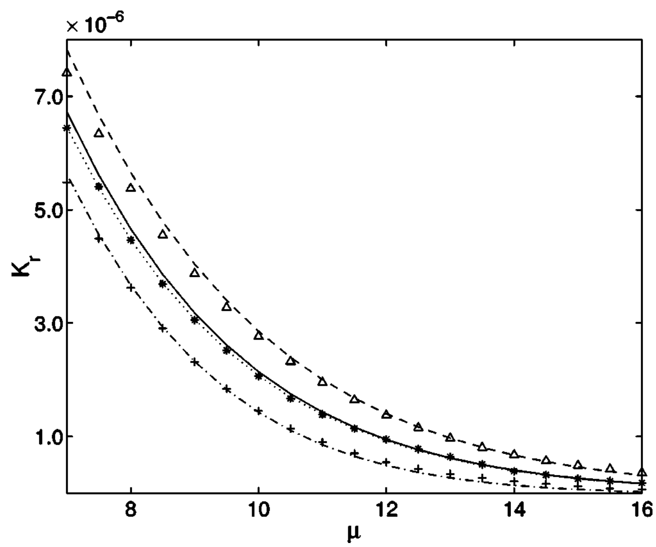

FIG. 2. The escape rate vs μ for different chaotic fluctuations: $G^{(2)}$ map (dashed curve-analytical expression; Δ markers-numerical simulation), Ulam map (dashed-dotted curve-analytical expression; + markers-numerical simulation), $G^{(3)}$ map (dotted curve-numerical simulation), and $G^{(4)}$ map (* markers-numerical simulation). Kramers' rate is given by the solid curve. The parameters employed are: $\tau=1.0$, $\gamma=2\times10^4$, $kT=2.0$. An ensemble size of 1×10^5 is used for the numerical simulations

from (10), depends on the magnitude of τ/γ, the form of the potential, and the noise intensity. By increasing τ, deterministic correlations become dominant. The consequence is a progressive desymmetrization of the distribution, which leads to an increase in activation rate beyond the standard Kramers rate. This interesting feature is clearly depicted in Fig. 1, where numerical results are shown to closely match the theoretical outcomes, especially when $\tau/\gamma \to 0$. Note that the escape rate from numerical simulations is obtained from the QKP map, with $K_r = (2t_{\mathrm{MFPT}})^{-1}$, where t_{MFPT} is the mean first-passage time [2]. In addition, the direction in which the Maxwell–Boltzmann distribution is desymmetrized depends on the sign of the odd-order correlations. For example, by using the Ulam map, which possesses odd-order correlations of opposite sign to those of the $G^{(2)}$ map, the distribution is desymmetrized in the opposite direction. The overall effect is a suppression of the escape rate given by $K_r = (1-A) \times (\omega/2\pi\gamma)\exp(-\mu/kT)$, with $\tau/\gamma < 9(kT)^3/(16\mu^4)$ [cf. Fig. 2]. Such statistical asymmetric effects may be experimentally validated by optically trapping dielectric glass beads in a turbulent environment [25,10].

Interestingly, although statistical asymmetry has led to a deviation from Kramers' rate, Eq. (12) shows that K_r converges to the Kramers escape rate for the class of even-order Tchebyscheff maps in the limit $\tau/\gamma \to 0$, as the particle distribution in the well converges to the Maxwell–Boltzmann distribution. However, the rate of convergence to the "symmetric state"—the Kramers escape rate, can be different for different even-order Tchebyscheff maps. For the $G^{(2)}$ map, the convergence rate scales in the order of $(\tau/\gamma)^{1/2}$, while for the $G^{(4)}$ map, we expect a more rapid rate of $O((\tau/\gamma)^{3/2})$ [12].

On the other hand, systems given by Eq. (14) with chaotic force from the class of odd-order Tchebyscheff maps can be considered as "symmetric" [21]. This is because the potential $V(x)$ appears symmetric to the ensemble of particles, if $\mu \gg kT$ and τ/γ is small. In consequence, no desymmetrization occurs, and we anticipate the escape rate to be the Kramers rate. Indeed, this is verified numerically for the case of $G^{(3)}$ map (see Fig. 2), where we have also found through numerical simulations that the distribution in the well is Maxwell–Boltzmann.

Finally, insights on the convergence to the Kramers escape rate can be understood from the perspective of a change in time scale. As τ approaches zero, Eq. (8) converges to the Smoluchowski equation with deterministic effects diminishing, while correlations which correspond to the white Gaussian model [18] gaining dominance. This expresses a fundamentally important notion that stochasticity, as apparent in many physical phenomena, may ultimately originate from a deterministic process that occurs at an infinitesimal time scale.

L.Y.C. gratefully acknowledges DSO National Laboratories for financial support.

[1] H. A. Kramers, Physica (Amsterdam) **7**, 284 (1940).
[2] P. Hänggi, P. Talkner, and M. Borkovec, Rev. Mod. Phys. **62**, 251 (1990).
[3] S. M. Soskin *et al.*, Phys. Rev. Lett. **86**, 1665 (2001); M. Arrayás *et al.*, *ibid.* **84**, 2556 (2000); I. Derényi and R. D. Astumian, *ibid.* **82**, 2623 (1999); V. I. Mel'nikov, Phys. Rep. **209**, 1 (1991).
[4] R. S. Maier and D. L. Stein, Phys. Rev. Lett. **86**, 3942 (2001); V. N. Smelyanskiy *et al.*, *ibid.* **82**, 3193 (1999); P. Reimann, *ibid.* **74**, 4576 (1995).
[5] R. D. Astumian and M. Bier, Phys. Rev. Lett. **72**, 1766 (1994); M. O. Magnasco, *ibid.* **71**, 1477 (1993).
[6] N. Agmon and J. J. Hopfield, J. Chem. Phys. **79**, 2042 (1983); J. Iwaniszewski, Phys. Rev. E **68**, 027105 (2003).
[7] I. Derényi *et al.*, Phys. Rev. Lett. **80**, 1473 (1998).
[8] C. Mennerat-Robilliard *et al.*, Phys. Rev. E **82**, 851 (1999).
[9] C. Nicolis and G. Nicolis, Phys. Rev. E **67**, 046211 (2003).
[10] C. Beck, Phys. Rev. E **49**, 3641 (1994); A. Hilgers and C. Beck, Europhys. Lett. **45**, 552 (1999).
[11] J. Rousselet *et al.*, Nature (London) **370**, 446 (1994); S. Leibler, *ibid.* **370**, 412 (1994).
[12] L. Y. Chew and C. Ting, Phys. Rev. E **69**, 031103 (2004).
[13] A. Hilgers and C. Beck, Phys. Rev. E **60**, 5385 (1999); C. Beck, Commun. Math. Phys. **130**, 51 (1990).
[14] H. Kantz *et al.*, Physica D **187**, 200 (2004).
[15] C. Beck, Physica A **169**, 324 (1990).
[16] H. Kantz and E. Olbrich, Physica A **253**, 105 (1998).
[17] C. Beck, in *Solitons and Chaos*, edited by I. Antoniou and F. Lambert (Springer, Berlin, 1991).
[18] A. Hilgers and C. Beck, Physica D **156**, 1 (2001); C. Beck, Nonlinearity **4**, 1131 (1991).
[19] C. Beck, Physica A **233**, 419 (1996).
[20] P. Hänggi *et al.*, Europhys. Lett. **35**, 315 (1996); D. R. Chialvo *et al.*, Phys. Rev. Lett. **78**, 1605 (1997).
[21] P. Reimann, Phys. Rev. Lett. **86**, 4992 (2001).
[22] C. Beck, J. Stat. Phys. **79**, 875 (1995).
[23] H. Risken, *The Fokker-Planck Equation* (Springer-Verlag, Berlin, 1989).
[24] P. Talkner, in *New Trends in Kramers' Reaction Rate Theory*, edited by P. Talkner and P. Hänggi (Kluwer, Dordrecht, 1995), p. 47.
[25] A. Simon and A. Libchaber, Phys. Rev. Lett. **68**, 3375 (1992).